Preprints (www.preprints.org) | NOT PEER-REVIEWED | Posted: 18 December 2017 doi:10.20944/preprints201712.0126.v1

Peer-reviewed version available at Sensors 2018, 18, 289; doi:10.3390/s18010289

Article

Design and Optimization of a MEMS-Based Piezoresistive Accelerometer for Head Injuries Monitoring: A Computational Analysis

Marco Messina [1,*], James Njuguna [2] and Chrysovalantis Palas [1]

[1] Maritime and Mechanical Engineering Department, Liverpool John Moores University, James Parsons Building Byrom Street, Liverpool, L3 3AF, UK; m.messina@ljmu.ac.uk
[2] Centre for Advanced Materials Engineering, School of Engineering, Robert Gordon University, Aberdeen, UK; j.njuguna@rgu.ac.uk
* Correspondence: m.messina@ljmu.ac.uk; Tel.: +44-151-231-2303

Abstract: This work focuses on the design improvement of a tri-axial piezoresistive accelerometer specifically designed for head injuries monitoring where medium-G impacts are common, for example in sports such as racing cars or American Football. The device requires the highest sensitivity achievable with a single proof mass approach, and a very low error (<1%) as the accuracy for these types of applications is paramount. The optimization method differs from previous work as it is based on the progressive increment of the sensor mass moment of inertia (MMI) in all three axes. The work numerically demonstrates that an increment of MMI determines an increment of device sensitivity with a simultaneous reduction of cross-talk in the particular axis under study. The final device shows a sensitivity increase of about 80% in the Z-axis and a reduction of cross-talk of 18% respect to state-of-art sensors available in the literature. Sensor design, modelling and optimization are presented, concluding the work with results, discussion and conclusion.

Keywords: piezoresistive accelerometer; sensor design; biomechanical device; head injuries monitoring; TBI

1. Introduction

One way of converting acceleration in an electrical signal is to deploy the piezoresistive effect. When the proof mass of an accelerometer is affected by inertial forces due to an external acceleration the strain/stress on the piezoresistors determines displacement that consequently produce a change in its resistance value proportionally to the acceleration applied to the device. Therefore, the voltage output will change accordingly and will represent, by less than a constant of proportionality, a measure of the acceleration.

Currently, when designing an acceleration sensor, the main struggle for designers is to find the right trade-off between sensor sensitivity and size, because the sensitivity significantly drops with size. Today's technology limits the size of an accelerometer below 1 square millimeter for the extreme loss in sensitivity [1, 2]. Clearly when miniaturization is an objective of the design, sensitivity become the main issue, because a reduced sensitivity will severely affect the device accuracy due to a low signal to noise ratio. In order to address this sensitivity problem a simple but not effective solution is to introduce an amplifier at the output level. This results into adding a further signal noise that certainly deteriorates the accuracy of the measurement.

This work aims at the design optimization of the mechanical structure of a piezoresistive accelerometer specifically designed for high performance traumatic brain injuries (TBI) measurements. The challenges faced in this particular design are miniaturization combined with high sensitivity and lowest possible cross-sensitivity (error from other axes of measurement). Notice that all the other sensor specifications, such as resolution, noise, temperature drift, etc. which are related to the electrical piezoresistors design, are not covered in this work as only the device mechanical

© 2017 by the author(s). Distributed under a Creative Commons CC BY license.

Preprints (www.preprints.org) | NOT PEER-REVIEWED | Posted: 18 December 2017 doi:10.20944/preprints201712.0126.v1

Peer-reviewed version available at Sensors 2018, 18, 289; doi:10.3390/s18010289

structure is studied here. The piezoresistors deployed for the sensor performance calculations are conventional micrometer devices.

When a head injury occurs, especially in helmeted sports such as race car accident, TBI are very common. In the past decade considerable research effort has been made in order to prevent and monitor the severity of head injuries, especially in motorsport. Many accidents and also deaths of race drivers occurred without any type of monitoring in the past, therefore, links between accelerations of specific body parts and injury could not be thoroughly made.

In the late 90s a first solution was introduced in the form of instrumented helmets mounting sensors measuring crash severity with the help of accelerometers. However, this solution was found not very appropriate because these instrumented helmets may not accurately measure the actual acceleration experienced by the head due to helmet-to-head fit and helmet liner properties [3-9]. Therefore, it was very difficult to estimate the acceleration forces passed to the head, because the helmets are designed to minimize the amount of acceleration experienced by the head, and in this way the acceleration measured by this technology may not reflect the acceleration of the head [10-12].

Further studies in this area suggest that for an accurate detection of head acceleration it is crucial the coupling between head and sensor, therefore the instrumented helmet solution has been soon replaced in the new century by a mouthpiece accelerometer in the football [13] and by an accelerometer attached to an earpiece and not to the helmet in the motorsport [14, 15]. These novel solutions allowed a direct and therefore more accurate assessment of the head acceleration.

In 2003 a version of these type of earpieces with an integrate acceleration sensor, called the Delphi Earpiece Sensor System (DESS) [16], was introduced for the first time in the Indy Racing League and Championship Auto Race Teams (CART). In 2006, a group of research at the Wayne State University leaded by Begeman [17] reported that these earplugs mounted in post mortem human specimens (PMHS) showed in the output signal a progressive phase lag from 50 to 100 Hz vibration when compared to skull measurement (rigidly mounted head accelerometers).

Furthermore, in 2009, Salzar et al. [18] explored a solution in order to try to avoid the issue found by Begeman earlier by developing a smaller tri-axial device meant to be placed inside the ear canal portion of the earpiece. The sensor showed improved coupling to the head over the DESS that was perceived too bulky [19]. Salzar adds that to further enhance the accuracy of the measurements it is advisable to improve the positioning technique and the mounting material, basically a stiffer material is recommended [18]. However, the sensor accuracy and miniaturization obtained by Salzar is not yet acceptable for this type of in-situ ear measurements. It is expected that an acceptable sensor error should be below 1% combined with a miniaturization below 2×2 mm^2.

In 2013, an attempt was made to improve earplug sensor sensitivity and miniaturization by integrating silicon nanowires as nanoscale piezoresistors. However, the manufacturing limitations harboured successful fabrication of a proof of concept [20], [21]. Finally, in 2014, a patent was published on a novel optimization method based on variation of the sensor mass moment of inertia [22], [23].

This work attempts a further improvement of the patented work [23] on earplug sensor technology by investigating a way of enhancing sensor performances and miniaturization by specific increments of the sensor mass moment of inertia (MMI), with the objective of achieving the most accurate response in case of medium-G impact crashes (<500G) not yet achieved in the state-of-art sensor design. The data gathered with a more accurate sensor would benefit all the stakeholders involved in the motorsport community and industry, for example by helping to design better drivers' car safety restraints systems, like shoulder harnesses, helmets, seat belts and head and neck restraints commonly used in all forms of racing.

Preprints (www.preprints.org) | NOT PEER-REVIEWED | Posted: 18 December 2017 doi:10.20944/preprints201712.0126.v1

Peer-reviewed version available at Sensors 2018, 18, 289; doi:10.3390/s18010289

2. Method

2.1. Piezoresistance

The piezoresistive effect is expressed by a matrix where each of the six fractional resistivity changes relates to each of the six stress components [1]. Kanda [2] general equation of the fractional resistivity change is as in equation (1) and mathematically this produce a matrix of 36 coefficients [1]:

$$\frac{\Delta\rho_\omega}{\rho} = \sum_{\lambda=1}^{6} \pi_{\omega\lambda} * \sigma_\lambda \quad (1)$$

where ω is a fixed voltage and current orientation and λ the stress orientation.

The coefficient are called piezoresistance coefficients, $\pi_{\omega\lambda}$, (ω, λ = 1 to 6), and are expressed in Pa^{-1}.

Typically, each piezoresistor has two contacts that are made by masked-ion implantation method and located on the beam, which is a very thin surface layer [3]. Thus, for the purpose of calculation only two piezoresistive coefficients are relevant, i.e. π'_{11} and π'_{12}. In the particular case that the stress is parallel with the direction of electric field and current density it is used π'_{11}, that is called the longitudinal piezoresistance coefficient, denoted by π_l. Likewise, in case the applied stress is perpendicular to the electric field and current density it is used π'_{12}, therefore called transverse piezoresistance coefficient, π_t. The shearing stress is neglected since it is much smaller than the others.

Mason [4] expressed these two coefficients through three fundamental piezoresistance coefficients π_{11}, π_{12}, π_{44}, and directional cosines (l, m, n) for arbitrary crystal orientation by the general simplification for longitudinal ($\pi_l = \pi'_{11}$) and transversal ($\pi_t = \pi'_{12}$) piezoresistive coefficient by:

$$\pi'_{11} = \pi_{11} - 2\pi_o(l_1^2 m_1^2 + l_1^2 n_1^2 + m_1^2 n_1^2) \quad (2)$$

$$\pi'_{12} = \pi_{12} - \pi_o(l_1^2 l_2^2 + m_1^2 m_2^2 + n_1^2 n_2^2) \quad (3)$$

$$(\pi_o = \pi_{11} - \pi_{12} - \pi_{44}) \quad \text{and} \quad \pi'_{12} = \pi'_{21} \quad (4)$$

Thanks to the theory and equations above, the resistance change becomes a function of the beam stress. This is true because in the real situation the piezoresistors are located on the thin beam surface, therefore at the surface plane the material is stressed mainly in two directions. Given the assumption that the mechanical stresses are constant over the piezoresistors, the fractional resistance change is given by:

$$\frac{\Delta R}{R} = \sigma_l \pi_l + \sigma_t \pi_t \quad (5)$$

where σ_l and σ_t are longitudinal and transversal stress.

It is worth noting that the equation (5) is only useable for uniform stress fields or if the piezoresistor dimensions are small compared to the beam size [1, 5].

Single crystal germanium and silicon are the first materials extensively used as piezoresistors since their diamond lattice crystal structure. In 1954 Smith [6] tested these semiconductor crystals and for the first time a large piezoresistive effect was reported observing that this phenomenon is theoretically explained by the study undertaken by Bardeen and Shockley [7], and later Herring [8, 9]. The work of Smith allowed the measurement of piezoresistive coefficients for (100)-silicon wafer along the <100> and <110> crystal orientations. Shear piezoresistive coefficients were indirectly calculated whereas longitudinal and transverse coefficients were measured directly. In particular, Smith with these measurements fully determined the piezoresistive tensor at a resistivity of 7.8 Ω-cm at low p-Si concentration considering also the crystal symmetry. Finally, he found the p-type longitudinal piezoresistive coefficient in the [110]-direction at light boron concentrations (≈1.7×10^{15} cm^{-3}) to be fairly constant at 72×10^{-11} Pa^{-1}. Kanda later presented his results graphically [2].

From their findings it can be asserted that p-type piezoresistors have to be oriented along the <110> directions to measure stress in (100)-wafers and thus the piezoresistors should be either lined up or perpendicular to the wafer primary flat [10]. These piezoresistors orientations are used in this work, moreover, for calculation of sensor performance the piezoresistive coefficient used is the one

Preprints (www.preprints.org) | NOT PEER-REVIEWED | Posted: 18 December 2017 doi:10.20944/preprints201712.0126.v1

Peer-reviewed version available at Sensors 2018, 18, 289; doi:10.3390/s18010289

found by Smith [6] for p-type silicon (**Table 1.** Piezoresistivity components for single-crystal silicon under certain doping values.).

In reality the piezoresistive coefficients of single-crystal silicon are variable and dependent on the type of dopant [11], the doping concentration [11, 12], and the temperature of the wafer substrate [2, 11]. As a consequence, designers need to take into account temperature and doping concentrations at the design stage because many components of the π matrix (π_{11}, π_{12} and π_{44}) are affected in different ways. In particular, when the temperature and doping concentration increases the value of the piezoresistive coefficient decreases, and this behavior has been observed for both p- and n-type silicon. Under certain typical doping concentration and dopant types the values of π_{11}, π_{12} and π_{44} for single-crystalline silicon have been experimentally determined. **Table 1.** Piezoresistivity components for single-crystal silicon under certain doping values. below lists typical values for selected doping concentrations.

Table 1. Piezoresistivity components for single-crystal silicon under certain doping values.

Piezoresistive coefficient (10^{-11} Pa^{-1})	n-type (resistivity = 11.7 Ωcm)	p-type (resistivity = 7.8 Ωcm)
π_{11}	-102.2	6.6
π_{12}	53.4	-1.1
π_{44}	-13.6	138.1

However, generally speaking there are circumstances where all 36 coefficients in the matrix [π] may be nonzero [61] when referring to a Cartesian system of arbitrary orientation relative to the crystallographic axes. For silicon, if the x-, y-, and z-axes are not in line with <100> directions the matrix components change.

Instead, in specific conditions, where the piezoresistors points in <100>, <110> or <111> directions [50, 62] the effective longitudinal and transverse piezoresistive coefficients can be summarizes as in Table 2.

Table 2. Formula for transverse and longitudinal piezoresistive coefficient for various commonly encountered resistor configurations.

Direction of Strain	Direction of Current	Configuration	Piezoresistive Coefficient
<100>	<100>	Longitudinal	π_{11}
<100>	<010>	Transversal	π_{12}
<110>	<110>	Longitudinal	$(\pi_{11}+\pi_{12}+\pi_{44})/2$
<110>	<110>	Transversal	$(\pi_{11}+\pi_{12}-\pi_{44})/2$
<111>	<111>	Longitudinal	$(\pi_{11}+2\pi_{12}+\pi_{44})/2$

Replacing the results in **Table 1.** Piezoresistivity components for single-crystal silicon under certain doping values. into the formulas of the piezoresistive coefficients in **Error! Reference source not found.** an estimation of the fractional resistance change given in equation (5) for p-type and n-type piezoresistors in the <110> and <100> direction is achievable. For example, for n-type piezoresistors in the <100> direction with a resistivity of 11.7 Ω-cm the fractional resistance change is as follows:

$$\frac{\Delta R}{R} = \sigma_l \pi_{11} + \sigma_t \pi_{12} = -\sigma_l 102.2 + \sigma_t 53.4 \approx \sigma_l \pi_{11} - \sigma_t \frac{\pi_{11}}{2} = \pi_{11}\left(\sigma_l - \frac{\sigma_t}{2}\right) \quad (6)$$

As it can be seen from eq. (6) the fractional resistance change is only a function of the longitudinal piezoresistive coefficient and when the transversal stress is doubled, the longitudinal stress it is zero. Therefore this results shows the suitability of the n-type piezoresistors in the <100> direction for measuring acceleration when the main stress component is the longitudinal stress as in uniaxial stress

Preprints (www.preprints.org) | NOT PEER-REVIEWED | Posted: 18 December 2017 doi:10.20944/preprints201712.0126.v1

Peer-reviewed version available at Sensors 2018, 18, 289; doi:10.3390/s18010289

applications. Clearly the p-type piezoresistors in the same direction with a resistivity of 7.8 Ω-cm are not suitable for measurements given the very low piezoresistive coefficients.

Comparing the n-type piezoresistors in the <110> direction with a longitudinal coefficient of -31.2×10^{-11} Pa^{-1} and a transversal coefficient of -17.6×10^{-11} Pa^{-1}, it is concluded that this configuration is generally not preferred for measurements on the <100> direction.

Instead in the <110> direction p-type piezoresistors with a resistivity of 7.8 Ω-cm show a fractional resistance change as:

$$\frac{\Delta R}{R} = \sigma_l \frac{\pi_{44}}{2} - \sigma_t \frac{\pi_{44}}{2} = \frac{\pi_{44}}{2}(\sigma_l - \sigma_t) \quad (7)$$

where compared to the π_{44}, π_{11} and π_{12} are considered zero due to their very low value.

This is the preferred configuration used in this study mainly because p-type piezoresistors in the <110> direction is a convenient crystallographic orientation from a fabrication standpoint [13], moreover boron is the most common used dopant. In a (100)-oriented wafer the p-type piezoresistors in the <110> direction are perpendicular to each other, therefore it is possible from a design point of view to fabricate the piezoresistors in the X- and Y-axis pointing to the <110> direction and detect the in-plane acceleration by simple Wheatstone Bridges circuits.

2.2. Design, Modelling and Optimization

This section aims at the design, modelling and optimization of a 3-axial single square millimeter bio-mechanic piezoresistive accelerometer available from the literature as state-of-art device [14, 15] and presents mass moment of inertia results. This chosen device as starting point of the optimization process is a three-axial accelerometer with one single mass available for all axes of measurement and it is characterized by a cylindrical proof mass suspended by four octagonal beams fixed to an external frame (Figure 1) [14], [15]. As accurate measuring of head accelerations is an important aspect in predicting head injury, it is important that the measuring sensor be well-coupled to the head [16]. Therefore, the main requirements of this application are miniaturization (≈ 1.5×1.5 mm^2) and medium-G measurement range (<500G) to allow the accelerometer incorporation into an earpiece. Bandwidth specification of the device is not relevant in this study has it can be adjusted by changing the device size accordingly. Typically, the frequency response of a miniature device like the one under study is of 1 kHz, a smaller device will determine a higher bandwidth of frequency. In reality for the particular application under study where high speed impacts are common, long duration transient are usually measured, therefore very low signal frequencies are expected in the order of 0-0.5 Hz. These low frequencies responses down to DC (i.e. they respond to steady-state accelerations) are specifically detected using a piezoresistor pick-off technology. At frequencies close to 0 Hz, piezoelectric accelerometers cannot, when high accuracy is required, measure the acceleration that an object is subject to [17].

In order to fulfil these requirements high sensitivity is a paramount feature due to the small dimension of the device under study. Moreover minimizing the cross-axis sensitivity is also very important such that the acceleration measured on one axis is not mixed with errors coming from the other axes. As a rule of thumb cross-talks needs to be below 1% of the main signal coming out from the axis under stress in order to have an accurate measurement.

Preprints (www.preprints.org) | NOT PEER-REVIEWED | Posted: 18 December 2017 doi:10.20944/preprints201712.0126.v1

Peer-reviewed version available at Sensors 2018, 18, 289; doi:10.3390/s18010289

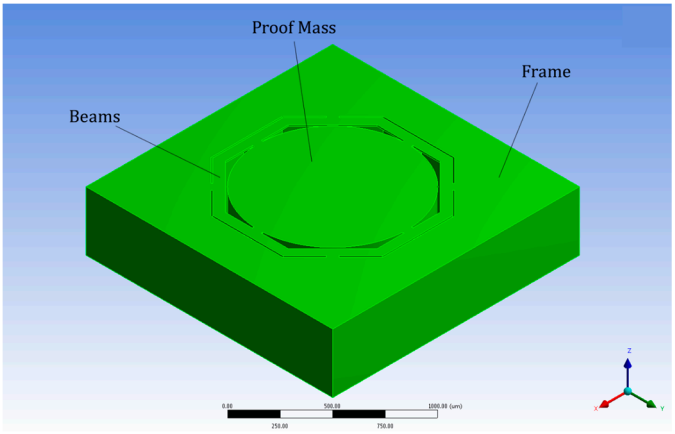

Figure 1. State-of-art mechanical structure of a three-axial accelerometer available in the literature [14, 15].

The optimization methodology adopted in order to increase sensor sensitivity and minimized cross-sensitivity is based on the hypothesis that an increment of sensor MMI will positively affect the sensor sensitivity and negatively influence the sensor cross sensitivity therefore overall improving sensor performance. The state-of-art sensor has been obtained from different optimization method based on MMI change as well [22, 23]. In this study the MMI will be increased progressively passing from a circular proof mass shape (Figure 1) to a cross shape, that, at each of the three iteration of optimization, increases the angle of curvature of the proof mass corners, until it becomes a complete cross as shown in Figure 2. The proof mass shape change from Circle to Cross 1 (top-right in Figure 2), and then to Cross 2 (bottom-right) and finally to Cross 3 (bottom-left).

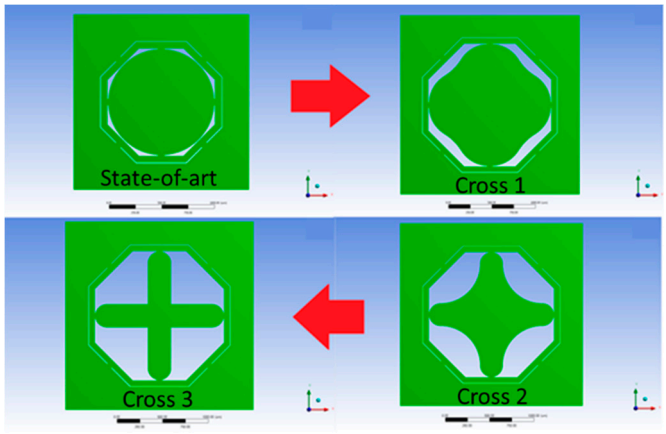

Figure 2. Mechanical structures top views. Optimization process that increases the MMI at each step of evolution and therefore hypothetically there would be an increase in the sensitivity and a reduction in cross sensitivity.

Hypothetically, this optimization would particularly increase the sensor sensitivity and minimized the cross-talk as the optimization reduced the distribution of mass on the biaxial area (XY-axis) but increases on the single axial area (X or Y-axis), therefore increasing the MMI at each step of the shape evolution.

Figure 3 shows the percentage increment of the MMI of each new shape in the X or Y-axis and in the Z-axis compared to the state-of-art shape (circle proof mass) available in the literature. As it can be seen, in order for the shapes to be comparable the proof mass volume of the pair of shape under study needs to be the same value.

Preprints (www.preprints.org) | NOT PEER-REVIEWED | Posted: 18 December 2017 doi:10.20944/preprints201712.0126.v1

Peer-reviewed version available at Sensors 2018, 18, 289; doi:10.3390/s18010289

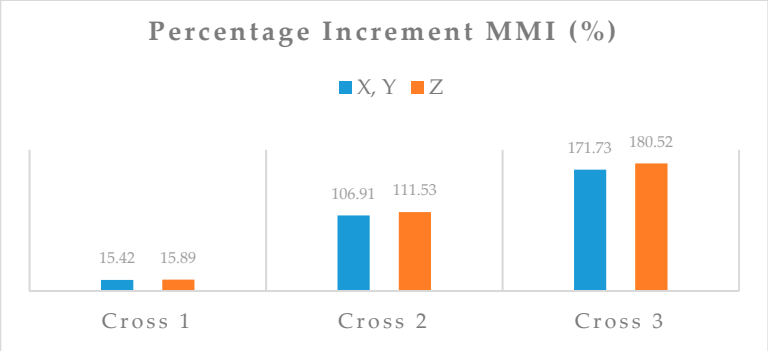

Figure 3. Percentage increment of MMI respect to state-of-art device. The shape Cross 3 offers the highest percentage increment of MMI.

2.3. Measurement Circuit

Wheatstone Bridge [18] is formed by four resistors connected in a quadrangle. The excitation that could be voltage or current is connected across one diagonal, whereas in the other diagonal there is a voltage detector. Basically the detector measures the voltage output difference of two dividers connected to the excitation [3]. There are different configuration of the bridge circuit, but the best one that minimize the nonlinearities and presents higher sensitivity is the full-bridge configuration which is also adopted in this study. In this configuration the voltage output is simply the excitation voltage times the fractional resistance change, as in (8).

$$V_{out} = V_{in} * \left(\frac{\Delta R}{R}\right) \quad (8)$$

In this work four piezoresistors are used for the full-bridge for the X- or Y-axis and eight piezoresistors are used for the Z-axis, therefore a total of 16 piezoresistors are used and placed in strategic locations on the top surface of the device mechanical structure (**Figure** -(a)). In particular these piezoresistors are placed where the highest stress is located by the stress simulation analysis in order to maximize sensor sensitivity. These regions are identified by finite element stress distribution analysis.

In Figure 4-(b) the three Wheatstone Bridges, specifically designed to maximize sensor sensitivity, are presented one for each axis that measure the output voltage drop. The bridges have some advantages, in fact, by using similar resistors the balanced configuration allows for temperature drift cancellation. Moreover, thanks to the particular sensor design used, which is the highly symmetric geometry, self-cancellation of part of the cross-axis acceleration is possible. That is why the piezoresistors are placed symmetrically one another.

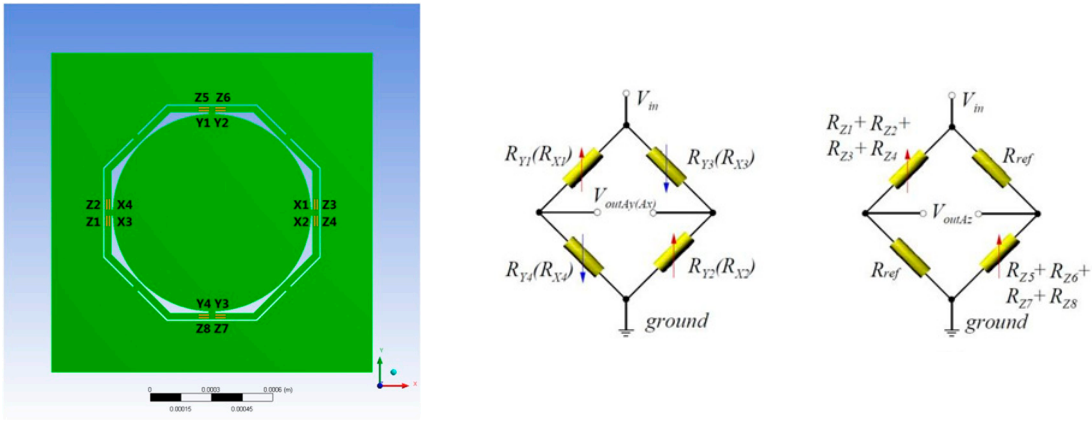

(**a**) (**b**)

Figure 4. Measurement Circuit design: (**a**) Piezoresistors location on the top surface of the device. A total of 16 piezoresistors are used, four for X-axis, four for Y-axis and eight for Z-axis; (**b**) Ax-, Ay- and Az-Wheatstone Bridge measurement circuit.

Preprints (www.preprints.org) | NOT PEER-REVIEWED | Posted: 18 December 2017 doi:10.20944/preprints201712.0126.v1

Peer-reviewed version available at Sensors 2018, 18, 289; doi:10.3390/s18010289

2.4. Electrical Sensitivity and Cross-Axis Sensitivity

In this work electrical sensitivity and cross-axis sensitivity have been selected as the mechanical structural parameters in order to measure the device performance. In the design of the micro-electro-mechanical device they give us information of accuracy and error in the measurements.

The accelerometer electrical sensitivity S is the ratio between the output voltage and the applied acceleration, as in (9). When there are in-plane acceleration (X- or Y-axis), the stress along the beams is perpendicular to the direction of the applied acceleration and represents the highest value respect to the stress distributed on the beam but parallel to the direction of the acceleration. Therefore, the piezoresistors to measure the acceleration on the X direction (Ax) are arranged on the Y-oriented beams, and vice versa. For example, for the Ax-bridge in the case of X-axis acceleration, the electrical sensitivity is [19]:

$$S_{Ax} = S_{Ay} = \frac{Vout_{Ax}}{A_x} = \frac{1}{A_x} * \frac{\Delta R_x}{R_x} * V_{in} \quad (9)$$

where V_{out} is the output voltage, V_{in} is the bias voltage applied to the piezoresistor (5V), and $\frac{\Delta Rx}{Rx}$ is the fractional resistance change of Ax-bridge that is equal to [1, 5]:

$$\frac{\Delta R_x}{R_x} = \pi_l * \sigma_l^y + \pi_t * (\sigma_t^x + \sigma_t^z) \quad (10)$$

where π_l and π_t are longitudinal and transverse piezoresistive coefficients respectively and $\sigma_l^y, \sigma_t^x, \sigma_t^z$, are respectively longitudinal stress in the Y-axis in case of acceleration along the X-axis, and transverse stress in the X- and Z-axis directions. The (10) is only valid for uniform stress fields or if the piezoresistor dimensions are small compared to the beam size [20].

Since the common approximation, where $\pi_l = -\pi_t$, is valid in the <110> silicon crystallographic direction, the fractional resistance change becomes:

$$\frac{\Delta R_x}{R_x} = \pi_l * [\sigma_l^y - (\sigma_t^x + \sigma_t^z)] \quad (11)$$

The electrical sensitivity in the other directions is similarly calculated. The longitudinal piezoresistive coefficient at room temperature used for the piezoresistor is 72×10^{-11} Pa^{-1} as reported by Smith [6].

Due to the sensor mechanical structure and fabrication errors that affect its symmetry, plus the not perfect piezoresistors symmetrical locations on the top surface and the inherent nonlinearities of the measurement circuit, there is an error of measurement related to these factors, called cross-sensitivity. Its sensitivity is calculated in percentage and it is the absolute value of the fraction of the voltage output of each axis other than the one under stress and the axis under stress. For example, the cross-axis sensitivities under the X-axis acceleration $S_{(Ax-Ay)\%}$ and $S_{(Ax-Az)\%}$ are detected, respectively, in the output of the Ay, Az-bridge for the piezoresistors as follows:

$$S_{(Ax-Ay)\%} = S_{(Ay-Ax)\%} = \left|\frac{Vout_{Ay}}{Vout_{Ax}}\right| \% \quad (12)$$

$$S_{(Ax-Az)\%} = \left|\frac{Vout_{Az}}{Vout_{Ax}}\right| \% \quad (13)$$

3. Results

3.1. Performance Calculation

Devices performance calculations are based on an extensive stress analysis carried out by Finite Element Method with solver available on ANSYS software package version 14.5. The number of nodes used for the meshing of shapes is about 250,000, moreover, the structures are fixed on the bottom frame and the load applied is an acceleration of 500G for each axis. Equation (7) correlates the stresses to the fractional resistance change. Data of stresses are then extracted from the simulation and sensitivity and cross sensitivity are eventually calculated.

Preprints (www.preprints.org) | NOT PEER-REVIEWED | Posted: 18 December 2017 doi:10.20944/preprints201712.0126.v1

Peer-reviewed version available at Sensors 2018, 18, 289; doi:10.3390/s18010289

In order to get the stresses values from the correct locations, a measurement circuit is developed with sixteen piezoresistors located where the highest stresses are detected to maximize the sensor electrical sensitivity (see **Figure** -(a)).

Sensitivity and cross-axis sensitivity have been calculated for the new shapes under study and compared to the state-of-art device shape. In **Error! Reference source not found.**5 the percentage sensitivity increment results for each new shape compared to the state-of-art device are presented.

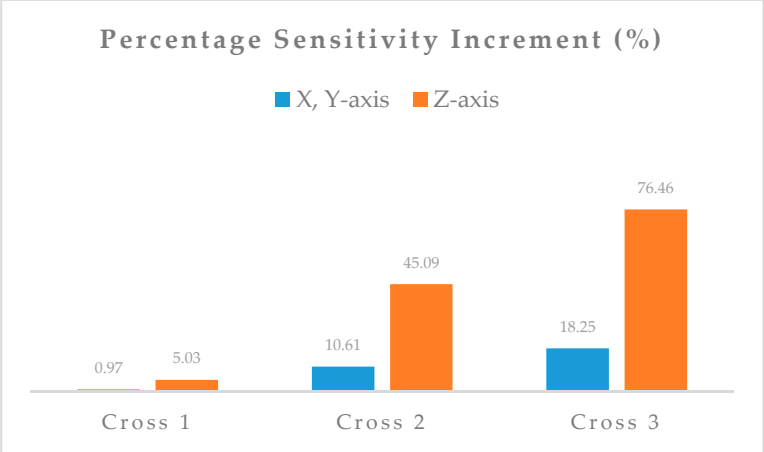

Figure 5. Sensitivity increment of new shapes in percentage. Highest increment is for the Z-axis sensitivity of shape Cross 3 (≈80%), overall the sensitivity increases progressively from shape Cross 1 to Cross 3, demonstrating the effect of MMI.

The progressive increment of sensitivity from shape Cross 1 to Cross 3 respect to state-of-art circle shape is down to the progressive increment of the MMI, therefore the study hypothesis is confirmed.

For example for shape Cross 3, an increment in the Z-axis of MMI of 180% determines a correspondent increment of sensitivity on the same axis of 76%.

Cross sensitivity of new shapes is expected also to reduce respect to circle shape as the distribution of masses around the corners in the cross shapes is reduced.

Figure presents the results of cross sensitivity of each new shape compared to state-of-art circle one. In the results there are three different values for circle shape as for each comparison the circle proof mass volume needed to be adjusted to the same volume of the new shape for simplicity of comparison. However, since the cross-axis sensitivity is given in percentage all shapes can be compared accordingly.

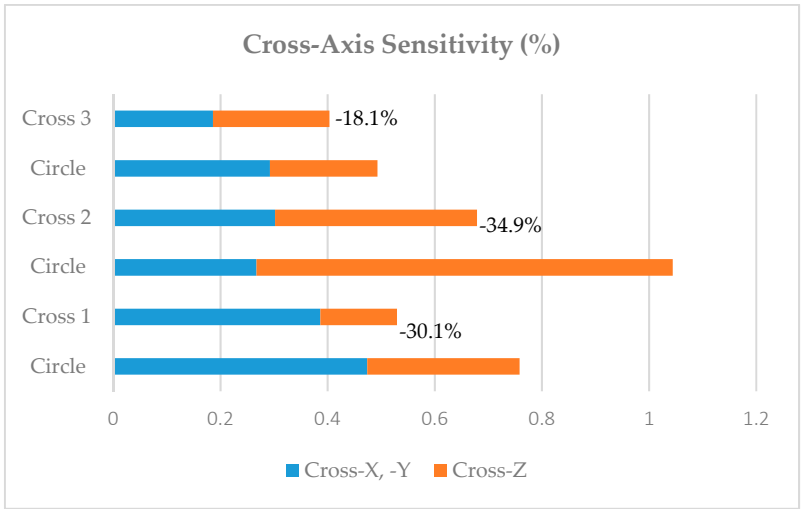

Figure 6. Cross-axis sensitivity reduction comparison of each new shape.

Preprints (www.preprints.org) | NOT PEER-REVIEWED | Posted: 18 December 2017 doi:10.20944/preprints201712.0126.v1

Peer-reviewed version available at Sensors 2018, 18, 289; doi:10.3390/s18010289

Lowest value of cross sensitivity as expected is of the new shape Cross 3, where the combined cross-X, or -Y, and -Z is of just 0.4%, well below the target of 1% for each axis.

4. Discussion

Comparing the optimized device performance to commercial devices, the only available three-axis medium-G accelerometer in the market, at the time of writing, are the analog 3×3mm² ADXL377 from Analog Devices Inc. specifically designed for concussion and head trauma detection with a range of ±200G (used currently in IndyCar races) and the digital 3×3mm² H3LIS331DL from STMicroelectronics with a maximum range of ±400G (used currently in Formula 1). The performance comparison is presented in the **Table 1**.

Table 1. Performance comparison with commercial devices.

Parameter	Cross 3 (this work)	ADXL377	H3LIS331DL
Measurement Range (G)	±500	±200	±400
Sensitivity (mV/G)	0.22	6.50	-
Cross-sensitivity (%FS)	<±1	±1.4	±2
Size (mm²)	1.5×1.5	3×3	3×3

The Cross 3 shape developed in this study is a 1.5×1.5 mm² device, therefore the sensitivity results reduced compared to the Analog Devices accelerometer that is 3×3mm². For a proper ear-plug device a 2×2mm² size is desirable as a bigger device would slip off the ear [21]. Moreover, the sensitivity of the ADXL377 is much higher of the device of this work as the signal output is amplified by internal circuitry, while the device developed in this work is not amplified at all.

Furthermore, the Cross 3 presents a higher measurement range because race car crash can reach impacts of more than 300G forces. Finally Cross 3 shape presents the lower cross-sensitivity of all three accelerometers, therefore is the most suitable device for biomechanical measurements. Notice that ST device sensitivity is not comparable as the device is digital. For this device the cross-sensitivity is ±2% for a range of ±70G, therefore for impacts of ±200G the error could reach peaks three times higher (≈±6%). Clearly this STMicroelectronics device is not suitable for biomechanical measurements as accurate measurements are necessary in case of head injuries and restraints systems design.

5. Conclusions

This work demonstrates the hypothesis that an increment of the MMI is a viable optimization method for a single mass mechanical structure of a piezoresistive accelerometer where high performance is a must, such as in biomechanical or biomedical applications. Examples are heart wall motion measurement for cardiac artificial pacemakers [22], hearing aid systems [23], and head injury monitoring of military soldiers in case of blast.

The increment of sensitivity of cross shapes respect to state-of-art circular shape reaches 76% in the Z-axis and 18% in the X- or Y-axis, moreover, the optimization method used allows for a simultaneously reduction of cross-axis sensitivity for the same shape of 18.1%. These results permit a higher accuracy of measurements respect to state-of-art devices in case high sensitivity and low error are paramount as in the head injuries monitoring. Future work will be to manufacture the optimal shape and test the performance under specified loading condition.

References

1. Barlian, A Alvin, Woo-Tae Park, Joseph R Mallon, Ali J Rastegar, and Beth L Pruitt. "Review: Semiconductor Piezoresistance for Microsystems." *Proceedings of the IEEE* 97, no. 3 (2009): 513-52.

Preprints (www.preprints.org) | NOT PEER-REVIEWED | Posted: 18 December 2017 doi:10.20944/preprints201712.0126.v1

Peer-reviewed version available at Sensors 2018, 18, 289; doi:10.3390/s18010289

2. Kanda, Yozo. "A Graphical Representation of the Piezoresistance Coefficients in Silicon." *IEEE Transactions on Electron Devices* 29, no. 1 (1982): 64-70.
3. Wilson, Jon S. *Sensor Technology Handbook*: Elsevier, 2004.
4. Mason, WP, JJ Forst, and LM Tornillo. "Recent Developments in Semiconductor Strain Transducers." *Semiconductor and conventional strain gauges* (1962).
5. Amarasinghe, R, DV Dao, VT Dau, BT Tung, and S Sugiyama. "Sensitivity Enhancement of Piezoresistive Micro Acceleration Sensors with Nanometer Stress Concentration Regions on Sensing Elements." Paper presented at the Solid-State Sensors, Actuators and Microsystems Conference, 2009. TRANSDUCERS 2009. International 2009.
6. Smith, Charles S. "Piezoresistance Effect in Germanium and Silicon." *Physical review* 94, no. 1 (1954): 42.
7. Bardeen, J, and W Shockley. "Deformation Potentials and Mobilities in Non-Polar Crystals." *Physical review* 80, no. 1 (1950): 72.
8. Herring, Conyers. "Transport Properties of a Many-Valley Semiconductor." *Bell Labs Technical Journal* 34, no. 2 (1955): 237-90.
9. Herring, Conyers, and Erich Vogt. "Transport and Deformation-Potential Theory for Many-Valley Semiconductors with Anisotropic Scattering." *Physical review* 101, no. 3 (1956): 944.
10. Maluf, Nadim. "An Introduction to Microelectromechanical Systems Engineering." IOP Publishing, 2002.
11. Tufte, ON, and EL Stelzer. "Piezoresistive Properties of Silicon Diffused Layers." *Journal of Applied Physics* 34, no. 2 (1963): 313-18.
12. Yamada, Kazuji, MOTOHISA Nishihara, Satoshi Shimada, MASANORI Tanabe, Michitaka Shimazoe, and Yoshitaka Matsuoka. "Nonlinearity of the Piezoresistance Effect of P-Type Silicon Diffused Layers." *IEEE Transactions on Electron Devices* 29, no. 1 (1982): 71-77.
13. Harkey, JA, and Thomas W Kenny. "1/F Noise Considerations for the Design and Process Optimization of Piezoresistive Cantilevers." *Journal of microelectromechanical systems* 9, no. 2 (2002): 226-35.
14. Messina, M, and J Njuguna. "High Performance Tri-Axial Piezoresistive Accelerometer." EP20120195830, Published by EPO, 2014.
15. Messina, M. Design and Optimization of a Novel Tri-Axial Miniature Ear-Plug Piezoresistive Accelerometer with Nanoscale Piezoresistors. PhD, Cranfield University, UK, 2013.
16. Begeman, Paul, John Melvin, Tara Troxel, and Andrew Mellor. "Frequency Response and Coupling of Earpiece Accelerometers in the Human Head." SAE Technical Paper, 2006.
17. Blejan, Marian, Ioana Ilie, Bogdan Lupu, and Mircea Comes. "Signal Conditioner for Piezoelectric Sensors." Paper presented at the Electronics Technology, 2008. ISSE'08. 31st International Spring Seminar on 2008.
18. Christie, S Hunter. "The Bakerian Lecture: Experimental Determination of the Laws of Magneto-Electric Induction in Different Masses of the Same Metal, and of Its Intensity in Different Metals." *Philosophical Transactions of the Royal Society of London* 123 (1833): 95-142.
19. Dao, Dzung Viet, Shigeya Okada, VT Dau, Toshiyuki Toriyama, and Susumu Sugiyama. "Development of a 3-Dof Silicon Piezoresistive Micro Accelerometer." Paper presented at the Micro-Nanomechatronics and Human Science, 2004 and The Fourth Symposium Micro-Nanomechatronics for Information-Based Society, 2004. Proceedings of the 2004 International Symposium on 2004.
20. Semiconductor, Freescale. "Accelerometer Terminology Guide" (2007), http://cache.freescale.com/files/sensors/doc/support_info/SENSORTERMSPG.pdf.
21. Salzar, Robert S, R Cameron, and Joseph A Pellettiere. "Improving Earpiece Accelerometer Coupling to the Head." *SAE International Journal of Passenger Cars-Mechanical Systems* 1, no. 2008-01-2978 (2008): 1367-81.

Preprints (www.preprints.org) | NOT PEER-REVIEWED | Posted: 18 December 2017 doi:10.20944/preprints201712.0126.v1

Peer-reviewed version available at Sensors 2018, 18, 289; doi:10.3390/s18010289

22. Lowrie, Craig, Marc PY Desmulliez, Lars Hoff, Ole Jakob Elle, and Erik Fosse. "Mems Three-Axis Accelerometer: Design, Fabrication and Application of Measuring Heart Wall Motion." Paper presented at the Design, Test, Integration & Packaging of MEMS/MOEMS, 2009. MEMS/MOEMS'09. Symposium on 2009.

23. Park, Woo-Tae, Kevin N O'Connor, Kuan-Lin Chen, Joseph R Mallon, Toshiki Maetani, Parmita Dalal, Rob N Candler, Vipin Ayanoor-Vitikkate, Joseph B Roberson, and Sunil Puria. "Ultraminiature Encapsulated Accelerometers as a Fully Implantable Sensor for Implantable Hearing Aids." *Biomedical Microdevices* 9, no. 6 (2007): 939-49.